RAPID COMMUNICATION

Adaptive genetic algorithm-based design of gamma-graphyne nanoribbon incorporating diamond-shaped segment with high thermoelectric conversion efficiency

Jingyuan Lu(陆静远)[1,2,†], Chunfeng Cui(崔春凤)[1,2,†], Tao Ouyang(欧阳滔)[1,2,‡], Jin Li(李金)[1,2], Chaoyu He(何朝宇)[1,2], Chao Tang(唐超)[1,2,§], and Jianxin Zhong(钟建新)[1,2]

[1] *School of Physics and Optoelectronics, Xiangtan University, Xiangtan* 411105, *China*
[2] *Hunan Key Laboratory for Micro-Nano Energy Materials and Device, Xiangtan University, Xiangtan* 411105, *China*

(Received 6 December 2022; revised manuscript received 4 January 2023; accepted manuscript online 31 January 2023)

The gamma-graphyne nanoribbons (γ-GYNRs) incorporating diamond-shaped segment (DSSs) with excellent thermoelectric properties are systematically investigated by combining nonequilibrium Green's functions with adaptive genetic algorithm. Our calculations show that the adaptive genetic algorithm is efficient and accurate in the process of identifying structures with excellent thermoelectric performance. In multiple rounds, an average of 476 candidates (only 2.88% of all 16512 candidate structures) are calculated to obtain the structures with extremely high thermoelectric conversion efficiency. The room temperature thermoelectric figure of merit (ZT) of the optimal γ-GYNR incorporating DSSs is 1.622, which is about 5.4 times higher than that of pristine γ-GYNR (length 23.693 nm and width 2.660 nm). The significant improvement of thermoelectric performance of the optimal γ-GYNR is mainly attributed to the maximum balance of inhibition of thermal conductance (proactive effect) and reduction of thermal power factor (side effect). Moreover, through exploration of the main variables affecting the genetic algorithm, it is revealed that the efficiency of the genetic algorithm can be improved by optimizing the initial population gene pool, selecting a higher individual retention rate and a lower mutation rate. The results presented in this paper validate the effectiveness of genetic algorithm in accelerating the exploration of γ-GYNRs with high thermoelectric conversion efficiency, and could provide a new development solution for carbon-based thermoelectric materials.

Keywords: adaptive genetic algorithm, thermoelectric material, diamond-like quantum dots, gamma-graphyne nanoribbon

PACS: 84.60.Rb, 72.15.Jf **DOI:** 10.1088/1674-1056/acb768

1. Introduction

Thermoelectric conversion, which could convert heat and electricity directly and reversibly, is a promising renewable technology for generating electricity and improving solid-state refrigeration by recovering waste heat (e.g., vehicle exhaust, exhaust gas from factory boilers).[1] Thermoelectric technology is one of the most potential candidates for new generation energy conversion, which could recover waste heat from energy consumption (e.g., automobile exhaust, exhaust gas from factory boilers) to available electricity.[2,3] For maximizing the thermoelectric performance, the material should host low thermal conductivity $(\kappa_e + \kappa_{ph})$, high electrical conductivity (σ), and large Seebeck coefficient (S).[4] The thermoelectric conversion efficiency could be evaluated by a dimensionless thermoelectric figure of merit (ZT): $ZT = \sigma S^2 T/(\kappa_e + \kappa_{ph})$. Because these parameters are coupled with each other, there encounter enormous difficulties in the process of exploring materials with high thermoelectric conversion efficiency.[5,6] Previously, traditional methods could improve the ZT values of materials by introduction of nanostructures,[7] defect engineering,[8] constructing quantum-well superlattice structures,[9] mixing with cement to make composite materials.[10–12] These methods indeed have made some progress in improving the thermoelectric conversion efficiency of materials. Nevertheless, these methods are generally based on random exploration pattern, and the cost of manpower and materials (or computational resources) is enormous during searching for a target structure with ideal thermoelectric performance. Therefore, it is particularly urgent and important to develop new technologies to solve these bottleneck problems.

In recent years, machine learning has attracted widespread attention in material design and prediction due to its advantages of accuracy, automation, rapidity, customizability, and scale;[10] for instance, employing Bayesian optimization to prediction of low-thermal-conductivity compounds,[13] using support vector machine, decision tree, random forest and gradient lifting decision tree to instruct single crystal growth[14] and sampling the equilibrium state of a multi-body

[†]These authors contributed equally to this work.
[‡]Corresponding author. E-mail: ouyangtao@xtu.edu.cn
[§]Corresponding author. E-mail: tang_chao@xtu.edu.cn

© 2023 Chinese Physical Society and IOP Publishing Ltd

system with deep learning.[15] The genetic algorithm appeared and adopted earlier, and its unique advantage is that it avoids the derivation process of the objective function value and can perform group search. It has been successfully applied in the structural design of thermoelectric materials based on machine learning.[16,17] Additionally, the algorithm is based on probabilistic rules combined with other techniques like neural network,[18] simulated annealing,[19] conjugate gradient,[20] making the search more flexible, scalable and applicable.[21] Genetic algorithm also has played a unique role in the field of thermoelectrics, e.g., exploring the hot-extruded process,[22] optimizing the thermoelectric generator,[17] searching stable structures,[23] planar torsional deformation.[24] Adaptive genetic algorithm improves on the basis of the classical genetic algorithm, and it has been continuously developed in recent years. The adaptive genetic algorithm could adjust the parameters according to the population to maintain the population diversity while ensuring the convergence of the algorithm, which is expected to demonstrate ground-breaking advances in the field of materials informatics.

Graphyne is one of the hottest points in the field of carbon nanomaterials research because of its unique structure, excellent optical and mechanical properties.[25–28] Such two-dimensional (2D) carbon structure constructed from both sp and sp^2 hybridized carbon atoms was firstly predicted by Baughman *et al.* as early as 1987.[29,30] In 2010 by using the coupling reaction under the catalysis of copper sheets, Li *et al.* successfully prepared large graphyne thin films.[25] After that, a variety production methods of graphyne have emerged.[31,32] Meanwhile, graphyne was also reported to host high Seebeck coefficient,[33] low thermal conductivity,[34] high carrier mobility,[35–37] and excellent thermal stability.[38–40] These natural advantages endow graphyne with great potential in the field of thermoelectric conversion.[34] Graphyne provides an ideal platform for the research of thermoelectric materials.

Motivated from the above description, taken gamma-graphyne nanoribbon (γ-GYNR) incorporating diamond-shaped segments (DSSs) as an example, the exploration of such structure with the excellent thermoelectric conversion efficiency is performed by using the adaptive genetic algorithm combined with nonequilibrium Green's functions method. The calculations show that genetic algorithm could efficiently identify the configuration with excellent thermoelectric conversion properties (the average number of times to obtain such structure with ZT greater than 99% $Z_{\max}T$ is 476, only account for the 2.88% of all structures). Moreover, the initial population gene pool, mutation rate, and individual retention rate are analyzed as well for modulating the optimization efficiency of the genetic algorithm. The paper is organized as follows. In Section 2, the structure of γ-GYNR incorporating DSSs is briefly introduced, as well as the methods used for research (basic content of genetic algorithm and calculation method of ZT). Section 3 verifies the effectiveness of the adaptive genetic algorithm optimization, systematically introduces the optimization results of the algorithm. Simultaneously, the effects of different parameters in the adaptive genetic algorithm are briefly analyzed and the physical mechanism of the excellent thermoelectric performance of the structure is analyzed. Finally, the above general work content is summed up.

2. Model and methods

The schematic of γ-GYNR incorporating DSSs is shown in Fig. 1. The system consists of two semi-infinite γ-GYNRs as leads and a central region with DSSs. In order to avoid the interaction between the leads and central region, buffer layers (2 unit cells) are set on both sides of the central region. Taking the diamond-shaped segment unit as "0" and the nanoribbons segment as "1", the diamond-shaped segment system can be converted into a binary code. According to this description method, the structure presented in Fig. 1 can be converted into binary codes [000110]. In our calculation, the diamond-shaped segment system with 15 units is studied, and the total number of candidate structures is 16512 (after considering the symmetry).

Genetic algorithm is an effective method based on Darwin's theory of biological evolution to simulate the natural evolution process for finding the optimal solution.[29] In order to facilitate the optimization, Geatpy[41] (a high-performance and practical evolutionary algorithm toolkit) is utilized to set up operators and participate in the construction of the basic framework of genetic algorithm. Adaptive genetic algorithm is a commonly used hybrid algorithm that adjusts its own parameters and makes it easier to jump out of local optimum.[42] Adaptive genetic algorithm has many applications in condensed matter field, such as crystal structure prediction,[43] and identifying a topological allotrope.[44] In this paper, the conventional mutation operator is changed into an adaptive mutation operator.

Figure 2 describe the flow chart for designing γ-GYNRs containing DSSs with excellent thermoelectric conversion efficiency using a combination of genetic algorithm. The framework of genetic algorithm in this paper is as follows. Initially, the random optimization method is used to combine a certain number of 15-bit binary codes randomly generated to obtain the first generation. The ZT values of these structures are calculated as the initial fitness function values. Then, the roulette wheel selection method is used as the selection method, and two-point cross recombination processing and mubin function (binary mutation operator) are used for mutation processing by means of the recombination function. The new offspring will be obtained as the parent to continue the natural selection until the desired target structure appears.

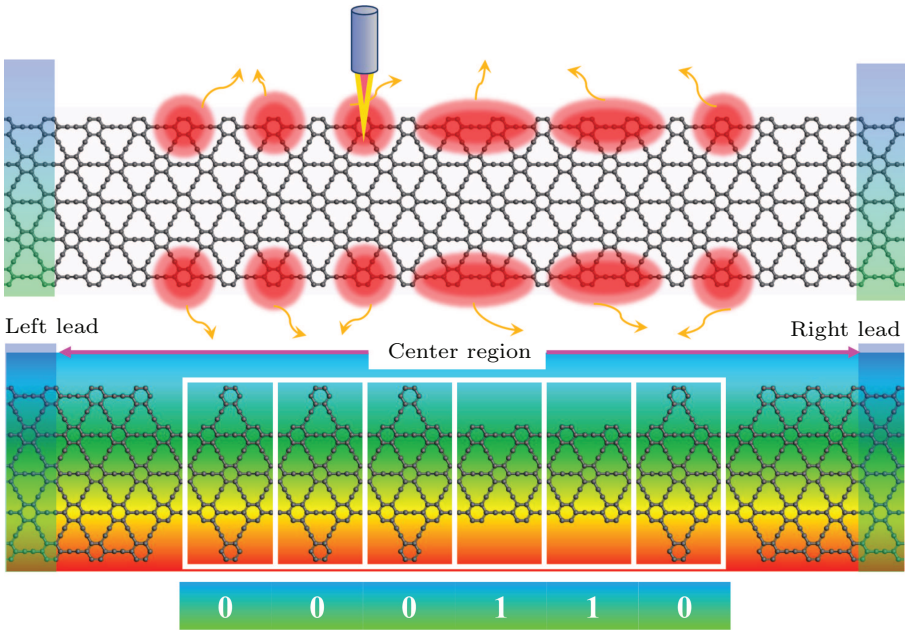


Fig. 1. The schematic diagram of the atomic structure of a γ-GYNR incorporating the diamond-shaped segments. The binary flags are selected as the descriptors: "1" and "0" for the nanoribbons segment and the diamond unit, respectively, and thus, the set of the descriptors for the example system is defined as [000110].

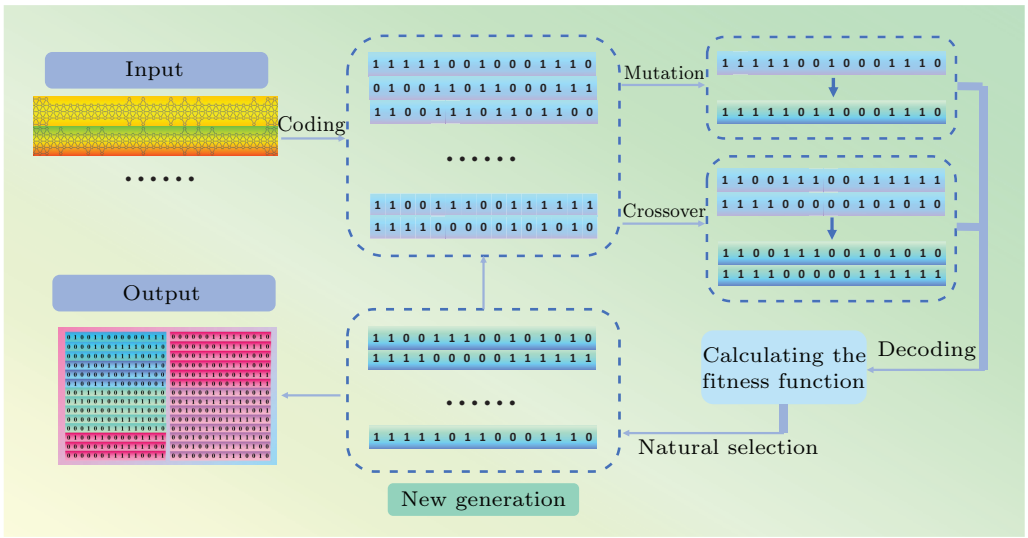


Fig. 2. Schematic design of γ-GYNRs incorporating DSSs with optimal thermoelectric conversion efficiency using a combination of genetic algorithm and nonequilibrium Green's function.

The adaptive process in this paper is to adjust the mutation rate according to the population's dissimilarity. The dissimilarity of two individuals is calculated as follows:

$$f(a,b) = \sum_{j=0}^{l-1} a_j \oplus b_j, \tag{1}$$

where l is the chromosome length, a_j is the jth gene on individual a chromosome, and b_j is the jth gene on individual b chromosome. The dissimilarity of population is given by

$$d_i = \frac{\sum_{i=0}^{N} \sum_{k=0,k\neq i}^{N} f(a_i,b_k)}{(N-1)\times(N-1)\times l} \times 100\%, \tag{2}$$

where N is the total number of individuals in the population, l is the length of individual chromosome. The greater the dissimilarity of a population, the better the diversity of the population and the richer the gene pool. Therefore, when the dissimilarity of population becomes small, the mutation rate should be increased to compensate for the evolutionary slowdown caused by the monotony of the gene pool. This adaptive genetic algorithm adjusts the mutation rate mainly according to the dissimilarity, which is 0.1 when the dissimilarity is greater than 0.16 and 0.2 when the dissimilarity is less than 0.16. The crossover rate is about 0.8, which is fine-tuned up or down in actual use.

In this process, the non-equilibrium Green's function is utilized to calculate the thermoelectric conversion effi-

ciency of γ-GYNRs incorporating DSSs, the calculation process is as follows.[5,45] Firstly, the free and open-source software GULP (General Utility Lattice Program)[46,47] with the second-generation reactive empirical bond order potential is employed to perform structural optimization on the whole candidate structures. Then, using the nearest-neighbor π-orbital tight-binding (TB) model, a Hamiltonian is constructed to calculate the transport properties of electrons. Based on the above model, the Hamiltonian matrix is written as

$$G^{\mathrm{r}}(E)=\left[(E+\mathrm{i}0^{+})I-H_{\mathrm{C}}-\Sigma_{\mathrm{L}}^{\mathrm{r}}-\Sigma_{\mathrm{R}}^{\mathrm{r}}\right]^{-1}, \tag{3}$$

where E present the energy of electrons, I is the identity matrix, H_{C} present the Hamiltonian in the central region, $\Sigma_{\mathrm{L(R)}}^{\mathrm{r}}(E)=H_{\mathrm{CL(R)}}g_{\mathrm{L(R)}}^{\mathrm{r}}H_{\mathrm{L(R)C}}$ present the self-energy of the electronic left or right lead.

The Lorentzian function can be used to solve the thermal conductivity σ contributed by the electron, the Seebeck coefficient S of the electron, the power factor P, and the thermal conductivity κ_{e} contributed by the electron, the formula is as follows:

$$L_n(u,T)=\frac{2}{h}\int_{-\infty}^{+\infty}(E-u)^n\left[-\frac{\partial f_{\mathrm{e}}(E,u,T)}{\partial E}\right]T_{\mathrm{e}}[E]\,\mathrm{d}E, \tag{4}$$

here, $f_{\mathrm{e}}(E,u,T)$ represents the Fermi–Dirac distribution at chemical potential μ and temperature T, and $T_{\mathrm{e}}[E]$ is the electron transport coefficient. The solution of the electron transport coefficient is a necessary step to calculate the Lorentz function. The calculation formula is

$$T_{\mathrm{e}}[E]=\mathrm{Tr}\left\{G^{\mathrm{r}}(E)\Gamma_{\mathrm{L}}G^{\mathrm{a}}(E)\Gamma_{\mathrm{R}}\right\}, \tag{5}$$

where $\Gamma_{\mathrm{L(R)}}=\mathrm{i}\left[\Sigma_{\mathrm{L(R)}}^{\mathrm{r}}(E)-\Sigma_{\mathrm{L(R)}}^{\mathrm{a}}(E)\right]$ represents the coupling function between the central region and left lead (right lead), $G^{\mathrm{a}}(E)=G^{\mathrm{r}}(E)^{\dagger}$.

The thermal conductivity contributed by the electron, the Seebeck coefficient S of the electron, the power factor P, and the thermal conductivity contributed by the electron are calculated as follows:

$$\sigma(u)=e^2L_0(u,T), \tag{6}$$

$$S(u)=\frac{1}{eT}\frac{L_1(u,T)}{L_0(u,T)}, \tag{7}$$

$$P(u,T)=S(u,T)^2\cdot\sigma(u,T), \tag{8}$$

$$\kappa_{\mathrm{e}}(u)=\frac{1}{T}\left[L_2(u,T)-\frac{L_1(u,T)^2}{L_0(u,T)}\right]. \tag{9}$$

The thermal conductivity of phonons is calculated in the similar way as electrons, the phononic retarded Green's function is

$$G^{\mathrm{r}}(\omega)=\left[(\omega+\mathrm{i}0^{+})I-K_{\mathrm{C}}-\Sigma_{\mathrm{L}}^{\mathrm{r}}-\Sigma_{\mathrm{R}}^{\mathrm{r}}\right]^{-1}, \tag{10}$$

the phonon transmission coefficient the lattice contribution to the thermal conductance $\kappa_{\mathrm{p}}(T)$ is defined as

$$T_{\mathrm{p}}[\omega]=\mathrm{Tr}\left\{G^{\mathrm{r}}(\omega)\Gamma_{\mathrm{L}}G^{\mathrm{a}}(\omega)\Gamma_{\mathrm{R}}\right\}, \tag{11}$$

$$\kappa_{\mathrm{p}}(T)=\frac{\hbar}{2\pi}\int_0^{\infty}T_{\mathrm{p}}(\omega)\omega\frac{\partial f_{\mathrm{p}}(\omega)}{\partial T}\,\mathrm{d}\omega, \tag{12}$$

here, $f_{\mathrm{p}}(\omega)$ represents the Bose–Einstein distribution function obeyed by phonons. Ultimately, by obtaining the above physical quantities, the thermoelectric conversion efficiency of the structure can be calculated by

$$ZT=\frac{\sigma S^2}{\kappa_{\mathrm{e}}+\kappa_{\mathrm{p}}}T. \tag{13}$$

3. Results and discussion

In this work, the γ-GYNRs incorporating DSSs (15 structural units) provide 16512 samples (considering symmetry) for the adaptive genetic algorithm to optimize the thermoelectric performance. To measure the stability of the algorithm, 10 rounds of calculations with different initial pools (all are randomly generated and optimized for combination) are executed to perform statistical averaging. In the meantime, to effectively measure the algorithm efficiency, in this work we define the ZT greater than 99% $Z_{\max}T$ as ZT_{ex}. In the initial generation, 180 structures are randomly selected, and the 20 individuals with the highest ZT values among them are chosen to form the first generation population. From Fig. 3, it can be clearly seen that within 1000 calculations (in the range of 200–900), the genetic algorithm can accurately find the structure with excellent thermoelectric conversion efficiency. Even in the worst round of optimization, only 890 calculations are needed to find the excellent structure accurately (only 5.40% of all 16512 candidate structures). In order to verify whether the results obtained by genetics match the actual ones, the ZT values of all candidate structures (16512) are computed in this paper. The results verify that the actual individuals with ZT_{ex} are consistent with the individuals with ZT_{ex} obtained by the genetic algorithm. There are three individuals with ZT_{ex}, the sets of binary structure descriptors are [010011000000111], [000010011110010], and [000000011110010]. The corresponding thermoelectric preferences are up to 1.622, 1.617, and 1.616 at room temperature, which are about 5.4 times higher than that of the original γ-GYNR (about 0.301). Additionally, the genetic algorithm optimization obtained other 28 potential candidate structures (structures with ZT higher than 95% $Z_{\max}T$, the corresponding binary structure descriptors are provided in the supplemental materials Section S2).

Taking the worst round of optimization process as an example, we exhibit the evolutionary process of thermoelectric conversion performance for each generation of samples, as shown in the inset of Fig. 3. It can be seen that the average of population's ZT has been continuously rising in each round,

and its rate of increase gradually slows down as the number of genetic generations increases. Meanwhile, the density closer to the $Z_{max}T$ is much greater than those farther away, and the ZT values of most individuals in the population are gradually approaching the optimal values. Furthermore, it can be found that new individuals with lower ZT continues to appear during the evolutionary process, which could keep the population genetic diversity.

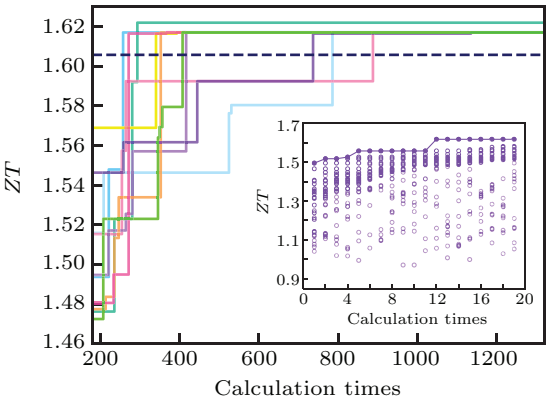


Fig. 3. The 10 rounds of optimization with different initial choices of structure candidates (above the dotted line is ZT_{ex}). The inset shows the scatter diagram of individual ZT composition for each unit as a reference (each unit contains 5 generations).

In order to illustrate the superiority of the adaptive genetic algorithm, the comparison between the computational results from the genetic algorithm (worst round of optimization) and random optimization is performed and the results are presented in Fig. 4(a). From the figure, one can note that the high-density region of the genetic algorithm is mainly scattered in the range of ZT from 1.1 to 1.4 (with an average highlight line with ZT about 1.3). The high-density region of the random optimization, however, is concentrated in a straight line with ZT about 1.1, obviously lower than the optimization results of the genetic algorithm. In order to analyze the overall distribution of ZT values for all individuals more clearly, a histogram of the frequency distribution of structural ZT values is provided in Fig. 4(c). It is clear that the ZT values obtained by the genetic algorithm are mainly distributed in the range of 1.105–1.435 (accounting for 75.9% of all individuals), with a median value of 1.255. While the ZT obtained by random optimization are mainly distributed in the range of 1.055–1.345 (accounting for 77.0% of all individuals), with a median value of 1.189. These results demonstrate the superiority of the genetic algorithm over the random optimization. Figure 4(d) depicts the N_{GA}/N_{Rand} obtained from ten sets of rounds with five typical regions of $ZT \geq 75\%\ Z_{max}T$, $80\%\ Z_{max}T$, $85\%\ Z_{max}T$, $90\%\ Z_{max}T$, and $95\%\ Z_{max}T$, here N_{GA} and N_{Rand} respectively denote the number structure candidates with specified ZT for the cases of genetic algorithm optimization and random optimization. As shown in Fig. 4(d), all the values of N_{GA}/N_{Rand} are larger than 1, indicating the genetic algorithm optimization is more effective and accurate than random optimization in all these 5 intervals. Furthermore, it can be seen that N_{GA}/N_{Rand} is significantly bigger than 1 in $90\%\ Z_{max}T$ and $95\%\ Z_{max}T$ and even up to 15, which suggests the genetic algorithm holding a significant advantage in obtaining the ZT in these two intervals. According to the results presented in both Figs. 3 and 4, one can conclude that the genetic algorithm optimization indeed possesses the robustness and usefulness in determining the structures with excellent thermoelectric conversion performance among all structures.

For revealing the physical mechanism behind the high thermoelectric conversion efficiency of γ-GYNR incorporating DSSs (length 23.693 nm and width 2.660 nm), we perform analysis on the thermoelectric transport properties. Here, we mainly focus on four configurations, i.e., pristine γ-GYNR, two periodic γ-GYNR incorporating diamond-shaped segment, and optimal structure (two periodic γ-GYNR incorporating DSSs and optimal structure descriptors are respectively [0000000000000000], [1111111111111111], and [0100110000001111]). As shown in Fig. 5(a), when the diamond-shaped segments are introduced into γ-GYNR, the electron transmission platform is destroyed, resulting in suppressed electron conductivity. The suppression of the electron transport arises from the electron scattering from the γ-graphyne diamond-shaped segment and the interface region in the diamond-shaped segment system. Meanwhile, it can be seen from Fig. 5(b) the maintenance of the band gap near the Fermi level and the emergence of new band gaps allow the Seebeck coefficient of γ-GYNR incorporating DSSs to be preserved and even slightly increased. That is to say, better thermoelectric properties can be obtained in more chemical potential regions for the γ-GYNR incorporating DSSs. From Fig. 5(c), one can note that the electronic thermal conductivity of the diamond-shaped segment system is significantly reduced as well with respect to the pristine case, and this result can also be explained from the fact that the thermal conductivity of electron contribution is proportional to the electron conductivity. To sum up the above, after introducing DSSs, the Seebeck coefficient of γ-GYNR increases, while the electronic conductance is decreased, accordingly a new physical quantity is needed to measure the situation. Thermal power factor is the product of the square of the Seebeck coefficient and the electronic conductance. As can be seen from Fig. 5(d), the thermal power factor is decreased compared to the pristine γ-GYNR. However, the decrease in the power factor of the optimal structure is not significant. At the same time, considering the electron-contributed thermal conductance is reduced as well, a maximum balance is needed to obtain a high ZT.

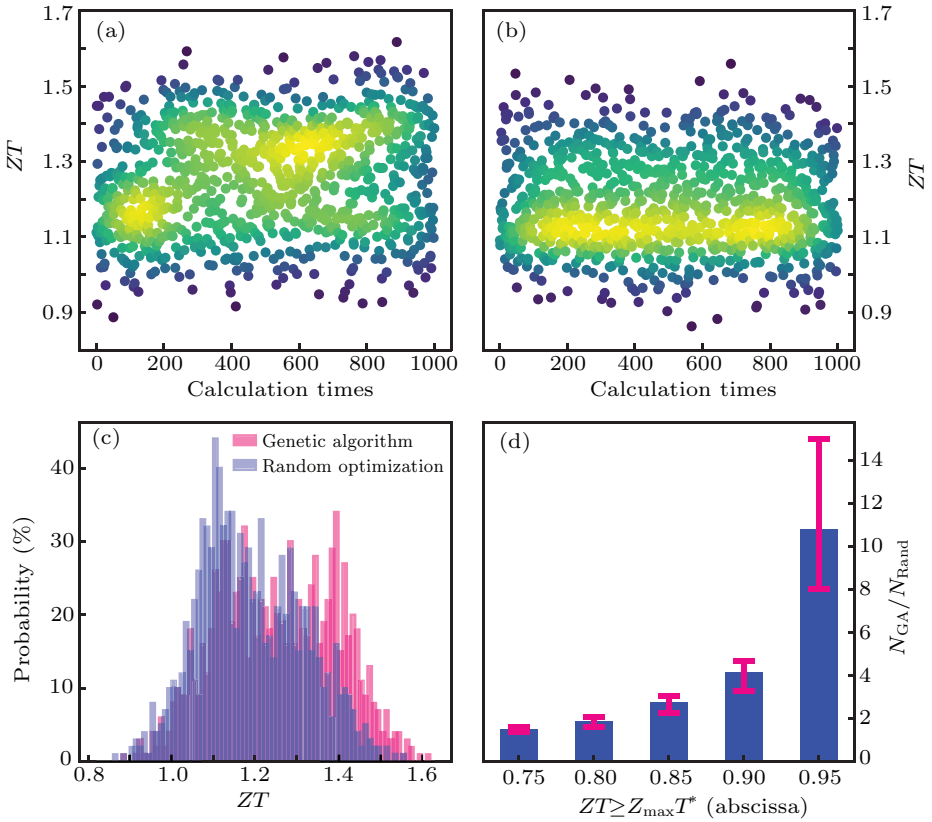


Fig. 4. In the worst round of genetic algorithm optimization and random optimization with the same optimization times (1000), (a)–(b) ZT values of optimized γ-GYNRs incorporating DSSs (the color of the dots in the scatter plot becomes lighter as the density increases), and (c) distribution of the ZT values of all optimized structures. (d) 10 groups of N_{GA}/N_{Rand} in five typical regions of $ZT \geq 75\%\ Z_{max}T$, $80\%\ Z_{max}T$, $85\%\ Z_{max}T$, $90\%\ Z_{max}T$, $95\%\ Z_{max}T$ ($Z_{max}T$ represents the highest ZT in all structure candidates).

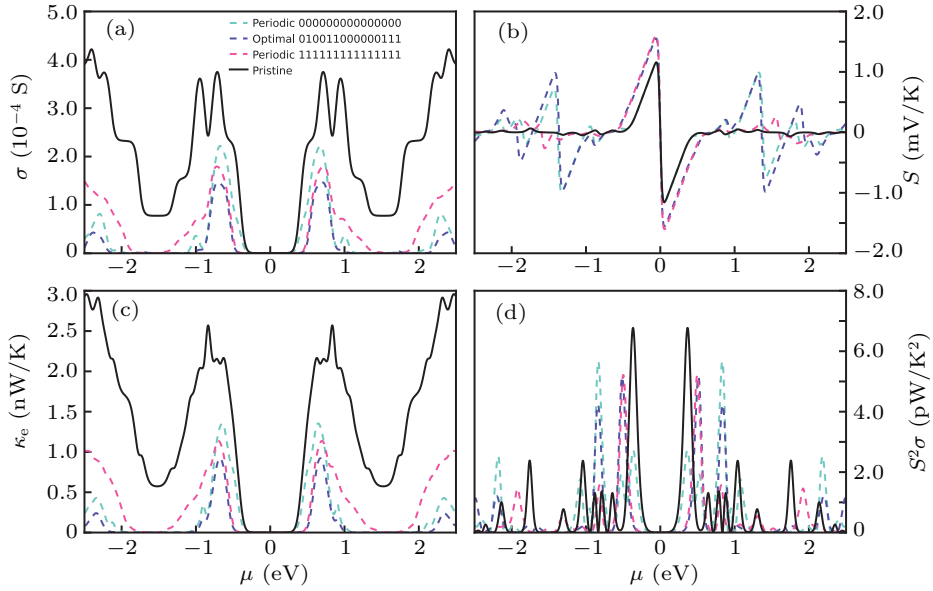


Fig. 5. At room temperature, the comparison of electronic transport properties of pristine γ-GYNR, two periodic γ-GYNR incorporating DSSs (structure descriptors: [000000000000000] and [111111111111111]) and optimal γ-GYNR incorporating DSSs (structure descriptor: [010011000000111]): (a) electronic conductance, (b) Seebeck coefficient, (c) electron-contributed thermal conductance, and (d) thermal power factor.

The phononic transport properties are also calculated for the above four structures, and the results are plotted in Fig. 6. Firstly, Fig. 6(a) depicts the phononic thermal conductivity of the four structures, and it is obviously that the introduction of the diamond-shaped segment will result in significant reduction of phononic thermal conductivity at all temperatures. At room temperature, the thermal conductivity of pristine γ-GYNR is 1.509 nW/K, which is much higher than that of the other three structures with diamond-shaped segment (0.438 nW/K, 0.322 nW/K, and 0.173 nW/K for the three structures of [000000000000000], [111111111111111], and [010011000000111], respectively), which plays a posi-

tive effect on improving the thermoelectric conversion efficiency. Similarly, one can see from Fig. 6(b) that the reduction in thermal conductivity is also reflected in phonon transport, where the phonon transport coefficients of pristine γ-GYNR show a clear quantization platform, which de-note the available transport channel for phonons. After introducing DSSs, phonon transport through the diamond-shaped segment encounters strong scattering and the quantitative platform is broken, giving rise to the suppressed phonon transport in the entire frequency range. To analyze the phonon transport more clearly, the phonon local density of states is calculated, and the results are depicted in Figs. 6(c)–6(e). For pristine γ-GYNR, the phonon states are uniformly distributed indicating that phonons can be successfully transported through the nanoribbon without any scattering. Figures 6(c) and 6(e) show the phonon local density of states of the periodic structure, where the uniform phonon states in the pristine γ-GYNR are disrupted due to scattering caused by the introduction of the diamond-shaped segment. However, some phonon channels could still be partially preserved. As for the optimal structure, one can find from Fig. 6(d) that the phonons are heavily blocked and scattered, and thus leading to a great suppression of phonon transport and a significant reduction of phononic thermal conductivity.

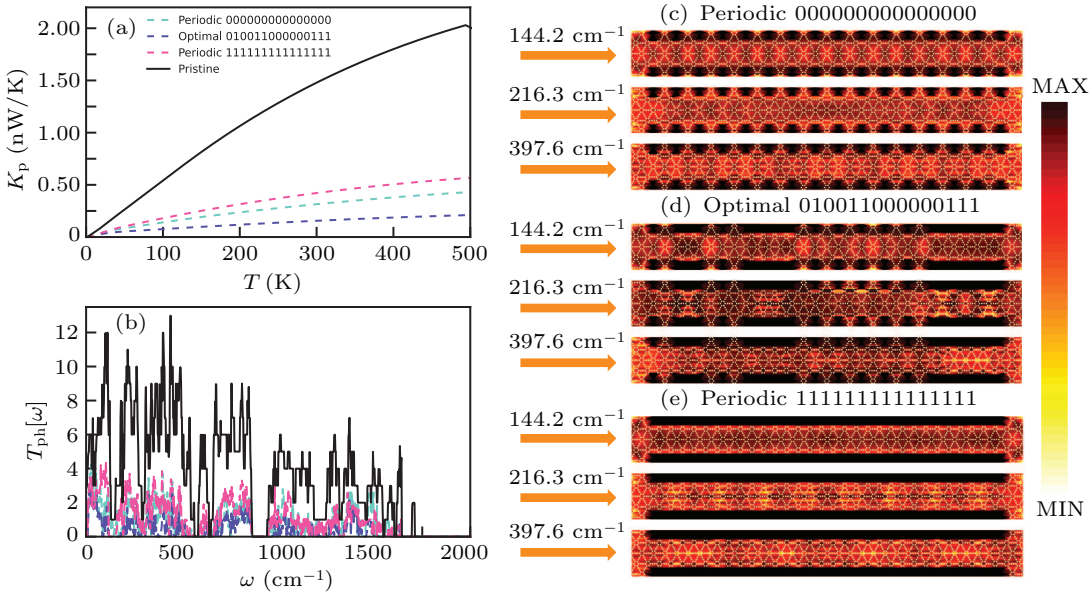


Fig. 6. The comparison of phononic transport properties of pristine γ-GYNR, two periodic γ-GYNR incorporating DSSs (structure descriptors: [000000000000000] and [111111111111111]) and optimal γ-GYNR incorporating DSSs (structure descriptor: [010011000000111]): (a) phonon-contributed thermal conductance, (b) phonon transmission coefficient, and (c)–(e) the phonon local density of states at three typical frequencies of 144.2 cm^{-1}, 216.3 cm^{-1}, and 397.6 cm^{-1}.

Based on the results presented in Figs. 5 and 6, one can conclude that the combined effect of the retained high Seebeck coefficient and largely suppressed phononic thermal conductivity finally lead to the boost of the thermoelectric performance of γ-GYNR incorporating DSSs. It is worth mentioning that the thermal power factor and thermal conductivity are coupled to each other based on the Mott's equation. Therefore, it is difficult to directly find the balance between these two variables only from the analysis of physical principles. However, genetic algorithm could solve such challenge by analyzing the correlation of the data, which significantly accelerates the structural optimization of the γ-GYNR.

Subsequently, we further analyze the key factors that affect the efficiency of teh genetic algorithm. In the optimization process, the following factors are need to adjust, e.g., the initial population gene pool, mutation rate, crossover rate, individual retention ratio, and number of individuals in the population. In this work, we mainly focus on the three key factors of the initial population gene pool, mutation rate, and individual retention ratio. In Fig. 7(a), the effect of the individual initial gene pool on the efficiency of the genetic algorithm is illustrated firstly. One can note that after the initial optimization of the initial individual gene pool (cyan bubble), the final optimized individual thermoelectric conversion efficiency is higher than 1.56 in all the cases, and the average ZT of the final genetic group is larger (indicated by the bubble area). Such result indicates that the individual initial gene pool optimization is beneficial to the evolution of the genetic algorithm. The mutation rate is investigated following, and the maxima ZT and dissimilarity of the final population are depicted in Figs. 7(b) and 7(c). It can be seen that in the process of adaptive genetic algorithm, individuals with ZT maxima less than 1.44 all have larger mutation rates, and the ZT maxima are generally greater than 1.46 when the mutation rate is 1%, 5%, and 10%. From Fig. 7(c), it can be found that the higher mutation rate, the greater evolved population's dissimilarity, i.e., the richer

genetic diversity. It is concluded that the mutation rate above a certain value will slow down the evolution of the population due to the high rate of loss of quality genes. From Fig. 7(d), one can find that when the retention rate is higher, the final average value of ZT is larger. However, after reaching a certain region, the retention ratio plays a minimal effect on the final ZT maximum obtained. In order to improve the efficiency of the genetic algorithm, we should perform initial optimization so that the original population genes remain high quality, and set a low mutation rate and high individual retention rate to retain the high quality genes.

For structures with different cell numbers, the efficiency of the genetic algorithm will be different. From the results presented in Fig. S2 of supplemental materials, one can find that as for the small system, the genetic algorithm does not possess superiority on identifying structures with excellent thermoelectric performance. That is to say, the larger the system the stronger the algorithm. To confirm the generalizability of the genetic algorithm, we chose defect gamma-graphyne nanoribbons for testing and the efficiency remained satisfactory. Test details are provided in the supplemental materials Section S3.

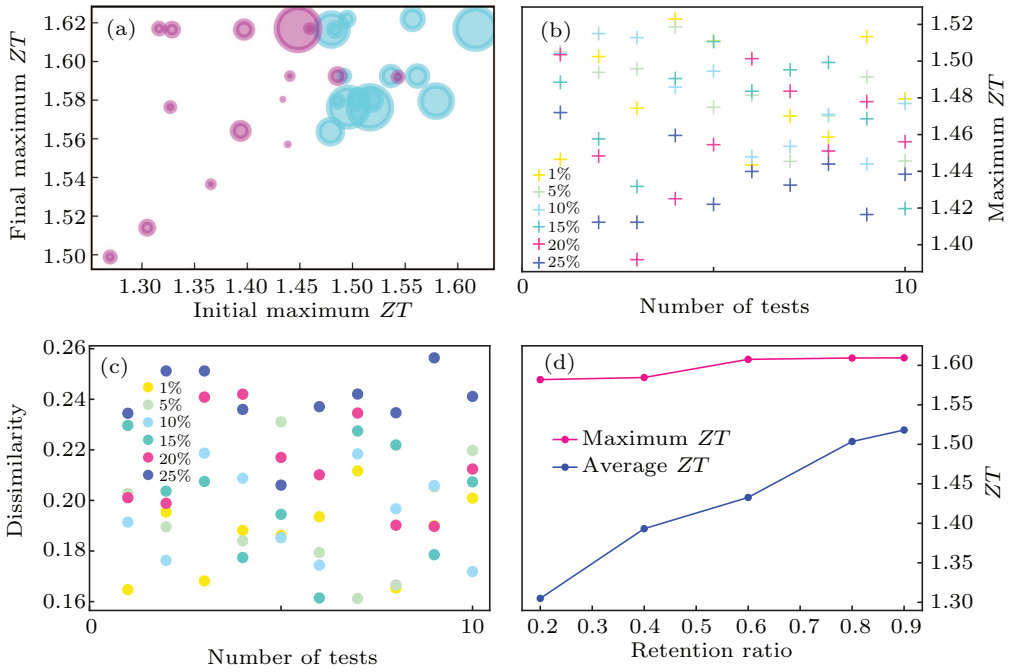


Fig. 7. (a) Maxima ZT and ZT average of populations after 800 calculations for different initial populations (cyan represents the initial optimization round, and pink represents the initial random round). (b) and (c) Maxima ZT and dissimilarity of populations after 500 calculations for different mutation rates (10 rounds each). (d) Maxima ZT and ZT average after 800 calculations for different retention ratios.

4. Conclusions

In summary, by means of nonequilibrium Green's function and adaptive genetic algorithm, we explore the optimal γ-GYNR incorporating DSSs with excellent thermoelectric conversion efficiency. The efficiency of optimization by genetic algorithm optimization far exceeds that of random optimization, even in the worst round, the average ZT after 1000 calculations is 1.251, which is obviously greater than the random optimization of 1.189. In the case of genetic algorithm optimization and random optimization, the number of structural individuals larger than a given ZT is greater than 1 for all groups in total rounds, and even reach more than 15 in the 95% $Z_{\max}T$ case. At room temperature, the ZT of the optimal γ-GYNR incorporating DSSs is calculated as high as 1.622, which is 5.4 times higher than that of pristine γ-GYNR. The high thermoelectric conversion efficiency of optimal γ-GYNR incorporating DSSs is mainly attributed to the maximum balance between the side effect of thermal power factor attenuation and the positive effect of thermal conductivity suppression. Additionally, we also investigate the effects of the initial population gene pool, mutation rate, and individual retention rate on the efficiency of the adaptive genetic algorithm. The results show that improving the quality of the initial population gene pool could greatly improve the efficiency of the genetic algorithm. Meanwhile, a higher individual retention rate and a lower mutation rate should be used for genetic algorithm optimization when the initial population is superior. The findings presented in this paper confirm the genetic algorithm indeed playing a viable role in the exploration of high thermoelectric conversion materials, and could provide guidance for the synthesis of nanocarbon-based thermoelectric devices. This work is performed under the framework of harmonic approximation, which may be inaccurate to describe longer structures (beyond the phonon mean free path). Therefore, we did not consider the calculation of longer gamma-graphyne nanoribbon. What is valuable is that we can indeed find the optimal

structure quickly and accurately using the adaptive genetic algorithm, and we still have a lot of related work to do in the future (for example, shape, width, doping, temperature of the structure).

Data availability statement

The data that support the findings of this study are available from the corresponding authors upon reasonable request.

Acknowledgements

Project supported by the National Natural Science Foundation of China (Grant Nos. 11974300, 11974299, and 12074150), the Natural Science Foundation of Hunan Province, China (Grant No. 2021JJ30645), Scientific Research Fund of Hunan Provincial Education Department (Grant Nos. 20K127, 20A503, and 20B582), Program for Changjiang Scholars and Innovative Research Team in University (Grant No. IRT13093), the Hunan Provincial Innovation Foundation for Postgraduate (Grant No. CX20220544), Youth Science and Technology Talent Project of Hunan Province, China (Grant No. 2022RC1197).

References

[1] Zhu T J, Zhao L D and Fu C U 2020 *Annalen Der Physik* **532** 2000435
[2] He J and Tritt T M 2017 *Science* **357** 6358
[3] Zhang W, Zhang X Q, Liu L, Wang Z Q and Li Z G 2021 *Chin. Phys. B* **30** 77405
[4] Snyder G J and Toberer E S 2008 *Nat. Mater.* **7** 105
[5] Yamamoto T and Watanabe K 2006 *Phys. Rev. Lett.* **96** 255503
[6] Xu Y, Xu X, Zhang W, Ouyang T and Tang C 2019 *Acta Phys. Sin.* **68** 247202 (in Chinese)
[7] Kim W, Zide J, Gossard A, Klenov D, Stemmer S, Shakouri A and Majumdar A 2006 *Phys. Rev. Lett.* **96** 045901
[8] Kim W, Lee W, Lee S M, Kim D and Park J 2022 *Nanotechnology* **33** 175702
[9] Broido and Reinecke 1995 *Phys. Rev. B* **51** 13797
[10] Maleki F, Ovens K, Najafian K, Forghani B, Reinhold C and Forghani R 2020 *Neuroimaging Clinics of North America* **30** E17
[11] Li Y N, Wu P, Zhang S P, Pei Y L, Yang J G, Chen S and Wang L 2022 *Chin. Phys. B* **31** 47203
[12] Cao Z, Fu Q Q, Gu H, Tian Z, Yaer X, Xing J J, Miao L, Wang X H, Liu H M and Wang J 2021 *Chin. Phys. B* **30** 97204
[13] Seko A, Togo A, Hayashi H, Tsuda K, Chaput L and Tanaka I 2015 *Phys. Rev. Lett.* **115** 205901
[14] Yao T S, Tang C Y, Yang M, Zhu K J, Yan D Y, Yi C J, Feng Z L, Lei H C, Li C H, Wang L, Wang L, Shi Y G, Sun Y J and Ding H 2019 *Chin. Phys. Lett.* **36** 068101
[15] Noé F, Olsson S, Köhler J and Wu H 2019 *Science* **365** 6457
[16] Wei H, Bao H and Ruan X L 2020 *Nano Energy* **71** 104619
[17] Sun H N, Ge Y, Liu W and Liu Z C 2019 *Energy* **171** 37
[18] Che Z G, Chiang T A and Che Z H 2011 *International Journal of Innovative Computing Information and Control* **7** 5839
[19] Djurisi A B, Elazar J M and Raki A D 1997 *Appl. Opt.* **36** 7097
[20] Cao R F, Pei X, Zheng H Q, Hu L Q and Wu Y C 2014 *Chinese Medical Journal* **127** 4152
[21] Katoch S, Chauhan S S and Kumar V 2021 *Multimedia Tools and Applications* **80** 8091
[22] Wang Z L, Adachi Y and Chen Z C 2020 *Advanced Theory and Simulations* **3** 1900197
[23] Xiong R, Sa B, Miao N, Li Y L, Zhou J, Pan Y, Wen C, Wu B and Sun Z 2017 *RSC Advances* **7** 8936
[24] Arabha S and Rajabpour A 2020 *Materials Today Commun.* **22** 100706
[25] Li G X, Li Y L, Liu H B, Guo Y B, Li Y J and Zhu D B 2010 *Chem. Commun.* **46** 3256
[26] Li C, Li J B, Wu F M, Li S S, Xia J B and Wang L W 2011 *Journal of Physical Chemistry C* **115** 23221
[27] Kang J, Li J, Wu F, Li S S and Xia J B 2011 *Journal of Physical Chemistry C* **115** 20466
[28] Pan L D, Zhang L Z, Song B Q, Du S X and Gao H J 2011 *Appl. Phys. Lett.* **98** 173102
[29] Baughman R H, Eckhardt H and Kertesz M 1987 *J. Chem. Phys.* **87** 6687
[30] Zhang Y Y, Pei Q X and Wang C M 2012 *Comput. Mater. Sci.* **65** 406
[31] Liu R, Gao X, Zhou J Y, Xu H, Li Z Z, Zhang S Q, Xie Z Q, Zhang J and Liu Z F 2017 *Adv. Mater.* **29** 1604665
[32] Yang C F, Li Y, Chen Y, Li Q D, Wu L L and Cui X L 2019 *Small* **15** 1804710
[33] Sevincli H and Sevik C 2014 *Appl. Phys. Lett.* **105** 223108
[34] Zhang Y Y, Pei Q X, Hu M and Zong Z 2015 *RSC Advances* **5** 65221
[35] Long M Q, Tang L, Wang D, Li Y L and Shuai Z G 2011 *ACS Nano* **5** 2593
[36] Jiang P H, Liu H J, Cheng L, Fan D D, Zhang J, Wei J, Liang J H and Shi J 2017 *Carbon* **113** 108
[37] Chen B, Li X Q, Xue L, Han Y, Yang Z and Zhang L L 2021 *Chin. Phys. B* **30** 57101
[38] Cranford S W and Buehler M J 2011 *Carbon* **49** 4111
[39] Narita N, Nagai S, Suzuki S and Nakao K 1998 *Phys. Rev. B* **58** 11009
[40] Hou X, Xie Z J, Li C M, Li G N and Chen Z Q 2018 *Materials* **11** 188
[41] Jazzbin E A 2020 http://www.geatpy.com/
[42] Jong D and Kenneth 1980 *IEEE Transactions on Systems, Man, and Cybernetics* **10** 566
[43] Wu S Q, Ji M, Wang C Z, Nguyen M C, Zhao X, Umemoto K, Wentzcovitch R M and Ho K M 2014 *J. Phys.: Condens. Matter* **26** 035402
[44] Zhan L J, Fang Y M, Zhang R T, Lu X C, Lu T Y, Cao X R, Zhu Z Z and Wu S Q 2022 *Phys. Chem. Chem. Phys.* **24** 15201
[45] Ouyang T and Hu M 2014 *Nanotechnology* **25** 245401
[46] Gale J D 2005 *Zeitschrift für Kristallographie - Crystalline Materials* **220** 552 DOI:
[47] Gale and D J 1997 *J. Chem. Soc.* **93** 629